Attachment 1

Reformatted Technical Report SIR-04-045, Revision 0

Report No.: SIR-04-045
Revision No.: 0
June 2004

Technical Report
Supporting the Palo Verde Pressurizer
Heater Sleeve Mid-Wall Repair

Prepared for:

Arizona Public Service Company

Prepared by:

Structural Integrity Associates, Inc.

Table of Contents

Section Page

1.0 BACKGROUND 1-1

2.0 INTRODUCTION 2-1

2.1 Objective 2-1
2.2 Licensing Change Summary 2-1
2.3 Repair Concept 2-1

3.0 ASME CODE EVALUATIONS 3-1

3.1 ASME Code, Section III Stress/Fatigue Evaluations 3-1
3.1.1 Load Definition 3-1
3.1.2 Stress Analyses 3-1
3.1.3 Load Combinations and Design Limitations 3-2
3.1.4 Fatigue Evaluations 3-3
3.2 ASME Code, Section XI Linear Elastic Fracture Mechanics Evaluations 3-3
3.2.1 Stress Analyses 3-3
3.2.2 Stress Intensity Factor Calculation Methodology 3-4
3.2.3 Calculated and Allowable Stress Intensity Factors 3-5
3.3 Elastic-Plastic Fracture Mechanics and Fatigue Crack Growth Evaluations 3-5
3.3.1 Material J-Resistance Curve 3-6
3.3.2 Calculation of Applied J-T 3-7
3.3.3 Fatigue Crack Growth Evaluations 3-9
3.4 Corrosion Evaluation of Pressurizer Base Material 3-9

4.0 CONCLUSIONS 4-1

5.0 REFERENCES 5-1

List of Tables

Table		Page
Table 3-1	Load Combinations	3-11
Table 3-2	Stress Criteria for ASME Code, Class 1 Components	3-11
Table 3-3	Transients	3-12
Table 3-4	Linearized Stress Intensity Results for Controlling Sleeve	3-12
Table 3-5	Primary Stress Intensity Evaluation	3-13
Table 3-6	Service Level A/B Load Combination Primary-Plus-Secondary Stress Intensity Evaluation	3-13
Table 3-7	Total Fatigue Usage for Option 1	3-14
Table 3-8	Total Fatigue Usage for Option 2	3-14
Table 3-9	Stress Intensity Factor Results	3-15
Table 3-10	J-T Instability Computations for Palo Verde Pressurizer Remnant Crack using ASME Code, Section XI, Appendix K Approximate Method, Initial Flaw Size of 0.6"	3-15
Table 3-11	J-T Instability Computations for Palo Verde Pressurizer Remnant Crack using ASME Code, Section XI, Appendix K Approximate Method, Extended Flaw Size of 1.2"	3-16
Table 3-12	Crack Growth Evaluation Cyclic Loads	3-16
Table 3-13	Stress Intensity Factor vs. Crack Size	3-17

List of Figures

Figure Page

Figure 1-1. Sketch of Palo Verde Pressurizer 1-2
Figure 2-1. Conceptual Drawing of Pressurizer Heater Sleeve Mid-Wall Repair 2-2
Figure 3-1. Finite Element Model 3-18
Figure 3-2. Row and Sleeve Numbering 3-19
Figure 3-3. Linearized Stress Paths for Sleeve Repairs 3-20
Figure 3-4. Crack Tip Element Location Definition 3-21
Figure 3-5. Schematic of EPFM Stability Analysis from ASME Code, Section XI, Appendix K 3-22
Figure 3-6. J-T Diagram for Several Reactor Vessel Steels and Welds Showing Rough Correlation with Charpy V-notch Upper Shelf Energy 3-23
Figure 3-7. Correlation of Coefficient C of Power Law J-R Curve Representation with Charpy V-notch Upper Shelf Energy 3-24
Figure 3-8. Correlation of Exponent m of Power Law J-R Curve Representation with Coefficient C and Flow Stress σ_0 3-25
Figure 3-9. J-T Diagram for EPFM Stability Analysis for Palo Verde Pressurizer Remnant Cracking Concern at a Flaw Size of 0.6" 3-26
Figure 3-10. J-T Diagram for EPFM Stability Analysis for Palo Verde Pressurizer Remnant Cracking Concern at a Flaw Size of 1.2" 3-26
Figure 3-11. Fatigue Crack Growth Results 3-27

EXECUTIVE SUMMARY

The pressurizer heater sleeves in the Combustion Engineering (CE) designed pressurized water reactors are made of Alloy 600 material which is welded to Alloy 82/182 weld metal, which is in turn welded to the low alloy steel pressurizer base material. These materials have been found to be susceptible to primary water stress corrosion cracking (PWSCC). Owners have taken one of two approaches in dealing with the adverse consequences of PWSCC in these materials, other than a complete pressurizer replacement. The first is to repair as problems arise, and the second is to take preemptive action. Arizona Public Service (APS) has chosen the latter approach.

An extensive pressurizer heater sleeve management study has been completed by APS. The study concluded that the appropriate technical and economical long term solution for Palo Verde is a repair method versus pressurizer replacement, particularly considering thirty-six (36) heater sleeves per unit. Palo Verde is, therefore, executing a pressurizer heater sleeve replacement program. The heater sleeves in Unit 2 were recently replaced (Fall 2003) during a steam generator replacement outage. A half-sleeve pad repair was implemented in Unit 2. A mechanical nozzle seal assembly has been utilized as an interim repair in the past until a permanent repair is prepared, planned and available for implementation on a wholesale and efficient basis.

This report describes a mid-wall repair technique that is a permanent solution to PWSCC in pressurizer heater sleeves. Stress analyses have been completed for the mid-wall repair and are summarized in this report. The analyses demonstrate that the repair satisfies all applicable construction code and licensing requirements. Fracture mechanics analyses have also been completed for leaving a flaw within the pressurizer vessel, and these analyses are also summarized in this report. A postulated flaw resides in a section of the original Alloy 600 heater sleeve and weld metal. The fracture mechanics analyses demonstrate that an assumed flaw left in place is acceptable for the life of the Palo Verde units, including a 20 year life extension. Similarly, a corrosion analysis has been performed for the crevice region between the sleeve and pressurizer base material. The analysis concludes that anticipated corrosion in the crevice region will be within code allowables, and is acceptable for the life of the plant, including a 20 year life extension.

1.0 BACKGROUND

The pressurizer is a vessel that is used to maintain and regulate system pressure in pressurized water reactors (PWRs). It contains water in the bottom and steam in the top of the vessel, and the fluid inside is heated to approximately 650°F, corresponding to a saturation pressure of approximately 2250 psia. To maintain the 650°F temperature, which is higher than the reactor vessel outlet (hot leg) temperature, there are thirty-six (36) pressurizer heaters in sleeves that penetrate the bottom head of the pressurizer. Figure 1-1 shows the Palo Verde pressurizer.

The heaters in CE designed plants are contained within sleeves made of Alloy 600 material and welded to Alloy 82/182 weld metal, which in turn was welded to the low alloy steel pressurizer base material. However, Alloy 600 material and associated weld metals (Alloy 82/182) have been found to be susceptible to PWSCC. These susceptible materials are present in all PWRs to some extent, and PWSCC has been observed previously in a number of locations, including reactor vessel top head control element drive mechanism nozzles and hot leg nozzles.

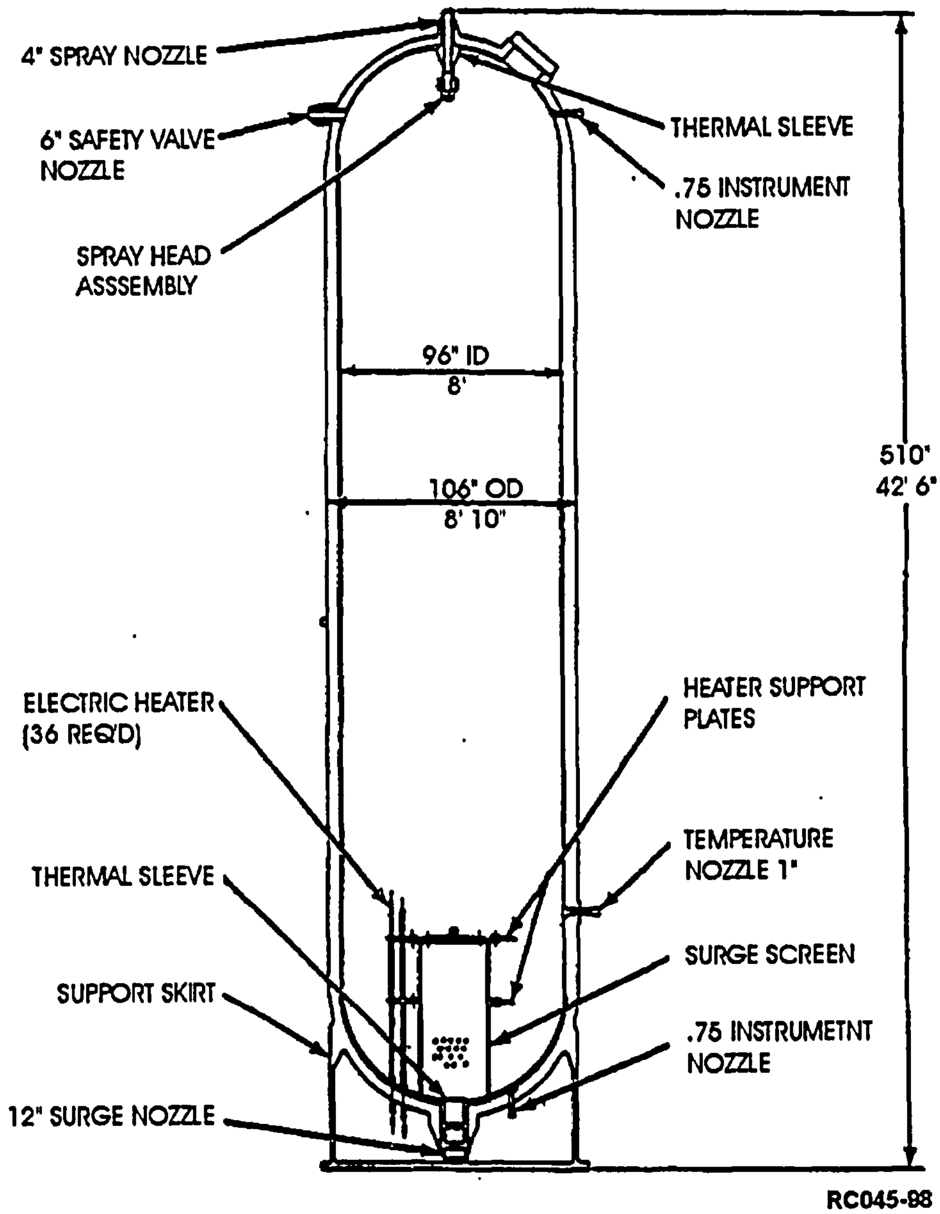

Figure 1-1. Sketch of Palo Verde Pressurizer

2.0 INTRODUCTION

2.1 Objective

The proposed mid-wall repair described in this document is a repair that can be implemented on a preemptive or emergent basis. The objective of this repair is to provide a permanent solution to PWSCC in pressurizer heater sleeves, incurring less radiation exposure and less expense than other repair methods. This report describes licensing issues and ASME Code evaluations associated with the mid-wall repair.

2.2 Licensing Change Summary

The mid-wall repair described in this report relocates the reactor coolant pressure boundary from a partial penetration weld on the inside surface of the pressurizer to a partial penetration weld at the mid-wall of the pressurizer. Figure 2-1 presents the concept. The repair design has been reviewed to ensure that it satisfies the design requirements of the ASME Code, Section III, for Class 1 components. Code Case N-638 was used as a guide in preparation of this document. Therefore, elevated temperature pre-heat, elevated temperature post-soak, and postweld heat treatment (PWHT) are not required.

The half sleeve mid-wall repair also leaves a postulated flaw within the pressurizer vessel. The flaw resides in a section of the original Alloy 600 heater sleeve and weld metal. This report contains fracture mechanics analyses that demonstrate that an assumed flaw left in place is acceptable for the life of the Palo Verde units, including a 20 year life extension. Similarly, a corrosion analysis has been performed for the crevice region between the sleeve and pressurizer base material. The analysis concludes that anticipated corrosion in the crevice region will be within code allowables, and is acceptable for the life of the plant, including a 20 year life extension. Since the fracture mechanics analyses utilize elastic-plastic fracture mechanics techniques, relief from some requirements of ASME Code, Section XI is required.

2.3 Repair Concept

The proposed mid-wall repair removes the lower section of the existing Alloy 600 heater sleeve. The new replacement heater sleeve is welded at about the mid-wall location to the inside of the vessel bore using the machine GTAW process and ambient temperature temperbead methodology. The reactor coolant system (RCS) pressure boundary is moved from the existing J-groove weld inside the vessel to the new mid-wall weld. A portion of the existing Alloy 600 sleeve (including the J-groove weld) is left in place. Figure 2-1 presents the concept.

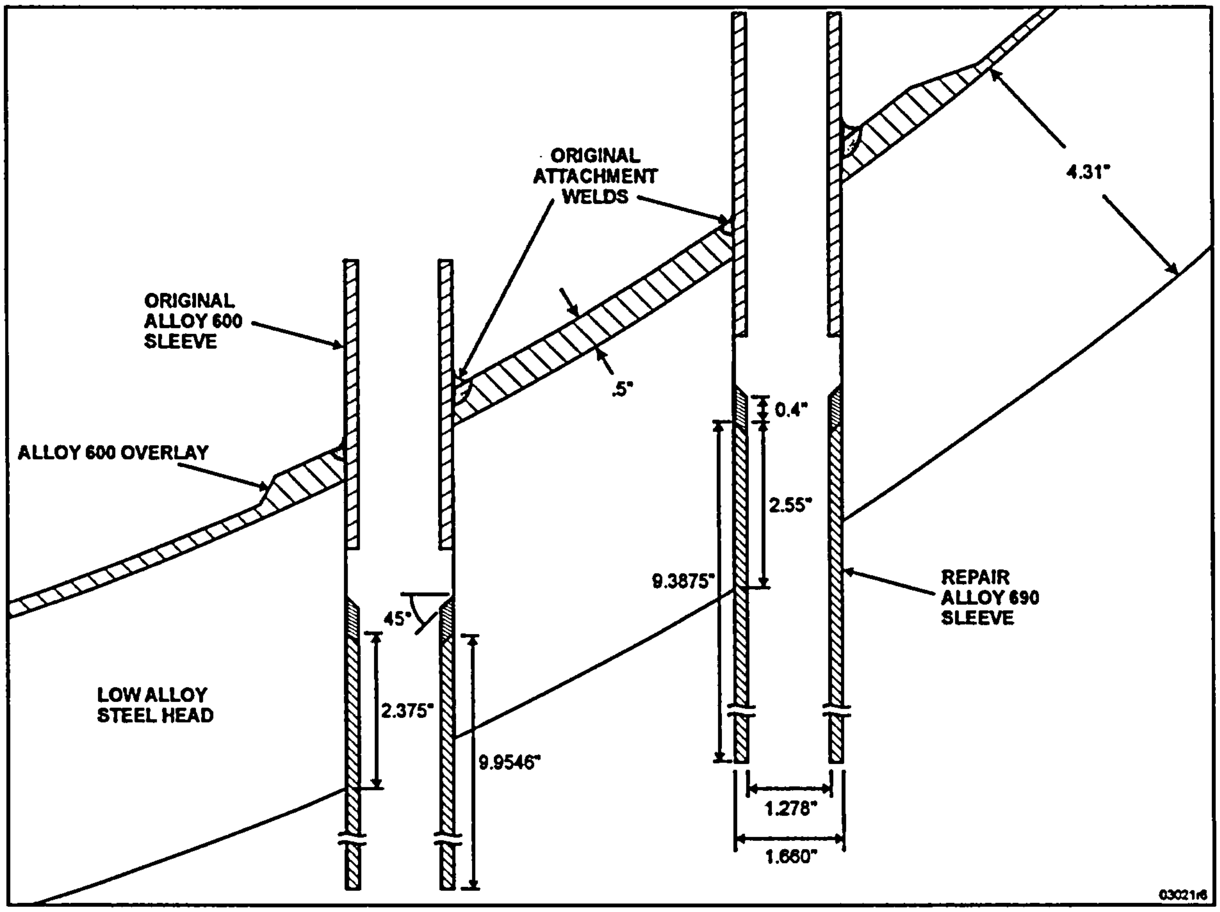

Figure 2-1. Conceptual Drawing of Pressurizer Heater Sleeve Mid-Wall Repair

3.0 ASME CODE EVALUATIONS

3.1 ASME Code, Section III Stress/Fatigue Evaluations

The requirements of Section III of the American Society of Mechanical Engineers (ASME) Boiler and Pressure Vessel Code must be met for the repair. Subarticle NB-3200 of Section III has limits on primary stress, primary-plus-secondary stress, and cumulative fatigue usage. Three-dimensional finite element analyses of the pressurizer bottom head region have been performed for application at Palo Verde. This section contains details of the analyses.

3.1.1 Load Definition

The analyses address original design basis conditions, as defined in the original Design Specifications. The Design Pressure for the pressurizer is 2500 psia, with a corresponding Design Temperature equal to 700°F. The normal operating pressure is 2250 psia, with a corresponding temperature of 653°F.

The following events were used in the analysis:

- Plant Leak Test at 2250 psia and 400°F
- Heatup and Cooldown at 200°F per hour
- Reactor Trip

The Reactor Trip transient also bounds the Loss of Reactor Coolant Flow and Loss of Load transients.

Table 3-1 defines the combinations of the basic loads that were examined, and Table 3-2 presents the allowable stress intensities for these load combinations. Table 3-3 summarizes the number of cycles associated with all transients considered in the design of the repair.

3.1.2 Stress Analyses

All stresses for this evaluation (aside from general closed-form solutions) were determined using a detailed three-dimensional finite element model, which was developed using the ANSYS computer program [1]. The model consists of the pressurizer lower head, a portion of the pressurizer cylinder, the support skirt, the surge nozzle and thermal sleeve, the instrument nozzle, the remaining portion of the original heater sleeves and the attachment J-groove/cover fillet welds, the new heater sleeves, and the new heater sleeve welds.

The dimensions of the repair were obtained from the sketch presented in Figure 2-1. Because of symmetry, a 90° model was used, with appropriate boundary conditions at the planes of symmetry. The model is shown in Figure 3-1. All components were modeled with three-dimensional isoparametric solid elements, which allows for refinement of the critical regions of the model.

A unit internal pressure load of 1,000 psi was evaluated. Stress results were then scaled to appropriate values by the ratio of the unit pressure load evaluated and the actual load occurring.

Thermal transient analyses were performed for the Heatup, Cooldown, and Reactor Trip, as described below. For these analyses, thermal boundary conditions were taken from the original pressurizer Stress Reports.

The Heatup transient begins at an initial uniform temperature of 70°F, followed by a ramp to 653°F at 200°F/hour. The maximum peak stress intensity occurred at 10,494 seconds into the transient.

The Cooldown transient starts at a steady state temperature of 653°F, then the internal fluid temperature drops to 70°F at a rate of 200°F/hour. The maximum peak stress intensity occurred at 4,408 seconds into the transient.

The Reactor Trip transient was modeled as two separate downward ramps followed by one upward ramp. The first downward ramp was from 653°F to 613°F over a total of 50 seconds. The second downward ramp was from 613°F to 593°F over a total of 550 seconds, followed by 400 seconds of an upward ramp to a temperature of 610°F. As maximum stresses were expected to occur near the steep portion of the transient, a total transient time of 1,000 seconds was used in the analysis. The maximum peak stress intensity occurred at 600 seconds into the transient.

The maximum membrane and membrane-plus-bending stress intensity results and their time of occurrence during the transients are shown in Table 3-4 for the controlling heater sleeve (see Figures 3-2 and 3-3 for sleeve and stress locations, respectively).

3.1.3 Load Combinations and Design Limitations

Subsubarticle NB-3220 of the ASME Code defines the stress limits that must be met for Class 1 components for all specified load combinations, as summarized in Table 3-2. To satisfy these limits, the maximum stress intensities for pressure and thermal effects at the various stress paths shown in Figure 3-3 were conservatively combined to determine the total stress intensities. The paths shown in Figure 3-3 represent a number of locations around the sleeves from 0° to 180° (for sleeves at the symmetric plane) or 0° to 360°.

For the Design, Service Level C/D, and Test Load Combinations, only primary stresses need to be evaluated. Hence, only pressure needs to be considered, as there are no other mechanical loads acting on the repair. The only material of consideration in the load combination is the Alloy 690 repair weld and sleeve. The allowable stress intensity (S_m) at 700°F for this material is 23.3 ksi. Note that since the original Code of Construction (the 1971 Edition of the ASME Code, through Winter 1973 Addenda [2]) does not have data on Alloy 690 material, the material data was provided by the 1989 Edition of the ASME Code [3].

Table 3-5 presents a summary of the stress intensities, and a comparison of the resulting stress intensities with the allowable values for the controlling sleeve. As can be seen from this table, all calculated stress intensities are less than their corresponding allowable values.

For the Service Level A/B Load Combination, only primary-plus-secondary stress intensities need to be evaluated. Table 3-6 summarizes the evaluation for the controlling sleeve. A very conservative load combination was used; the stress intensities of the operating pressure, cooldown thermal transient, and reactor trip thermal transient were summed to determine the range of stress intensity. As can be seen from Table 3-6, all locations have calculated stress intensities that are less than the allowable value for this load combination.

3.1.4 Fatigue Evaluations

Subsubparagraph NB-3222.4(e) of the ASME Code, as supplemented by Subparagraph NB-3228.5, requires the determination of the ability of components to withstand cyclic service. A fatigue evaluation was performed to assure that the repair satisfied the requirements of the ASME Code with respect to cyclic loads during service. The fatigue evaluation was performed for the path locations shown in Figure 3-3.

Table 3-3 presents the total number of cycles for the design life, including a 20 year life extension. To provide maximum confidence in the fatigue calculation, two methods of cyclic combination were investigated. The cyclic combinations for Option 1 and Option 2 are as follows:

Option 1:

- Cooldown+Trip+P_{Trip} (for a total of 720 cycles)
- Cooldown+Heatup+$P_{Operate}$ (for a total of 30 cycles)
- P_{leak} (for a total of 300 cycles)

Option 2

- Trip+$P_{Delta\ Trip}$ (for a total of 720 cycles)
- Heatup+Cooldown+$P_{Operate}$ (for a total of 750 cycles)
- P_{leak} (for a total of 300 cycles)

The total fatigue usage was obtained by summing the contributions from each of the three load combinations described above for the two options. Table 3-7 tabulates the fatigue usage for Option 1, while Table 3-8 tabulates the fatigue usage for Option 2. As can be seen in these tables, the cumulative fatigue usage factor is less than unity for all locations.

Based on the analysis results above, the requirements of Section III of the ASME Code have been satisfied.

3.2 ASME Code, Section XI Linear Elastic Fracture Mechanics Evaluations

Section XI of the ASME Code requires that any flaws that are not removed be analyzed for acceptability on fracture toughness and potential crack growth. Section XI provides acceptance criteria, and any flaw must be shown not to grow beyond an allowable flaw size within the remaining life of the plant. For purposes of this analysis, flaws were conservatively postulated on both the uphill and downhill sides in the remnant portion of the original sleeve, the original attachment welds, and the overlay material (see Figure 2-1).

3.2.1 Stress Analyses

As with the Section III analyses described in Section 3.1, three-dimensional finite element techniques were used in the fracture mechanics analyses, with crack face pressures input from the

Section III analyses. In addition to the Heatup, Cooldown, and Reactor Trip transients analyzed for the ASME Code, Section III analyses, the Loss of Secondary Pressure transient was analyzed as well for allowable flaw size. However, it was not used for the fatigue crack growth analysis since it is a Service Level C/D event.

3.2.2 Stress Intensity Factor Calculation Methodology

A finite element model, more detailed than that used in the stress analyses, was used to calculate stress intensity factors during the transients. The postulated cracks are located at both the uphill and downhill sides of the penetration, as shown in Figure 3-4. The model includes a crack in the entire cross-section of the J-groove weld, extending through the overlay material to the overlay/vessel interface, and a through-wall axial crack in the sleeve body. The postulated axial crack in the original sleeve body begins at the top of the sleeve and extends all the way to the bottom of the sleeve remnant.

Stresses from the stress analyses described above, in which the crack is not modeled, are input as pressures on the crack face, using a standard fracture mechanics superposition technique. This technique is based on the principle that in the linear elastic regime, stress intensity factors of the same mode, which are due to different loads, are additive, similarly to stress components in the same direction [4].

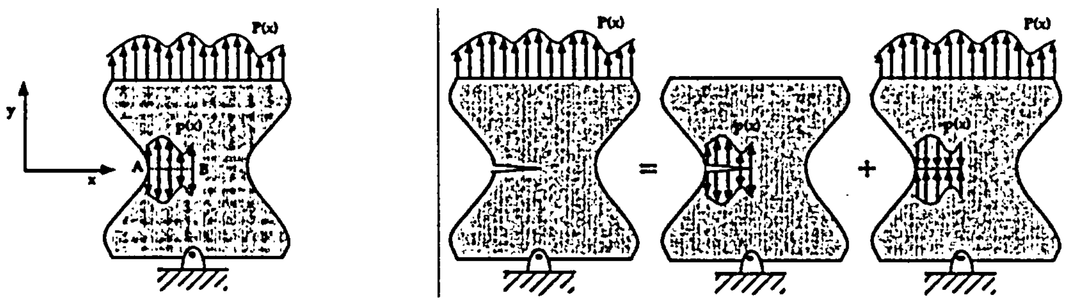

(a) (b) (c) (d)

A load P(x) on an uncracked body (Sketch (a)) produces a normal stress distribution p(x) on Plane A-B. Sketches (b), (c) and (d) show the same body with a crack at Plane A-B, and the stress intensity factors resulting from these loading cases are such that:

$$K_{I(b)} = K_{I(c)} + K_{I(d)}$$

Thus, since $K_{I(d)} = 0$ because the crack is closed,

$$K_{I(b)} = K_{I(c)}$$

This means that the stress intensity factor obtained from subjecting the cracked body to a nominal load P(x) equals the stress intensity factor resulting from loading the crack faces with the resulting stress distribution p(x) at the crack location in the uncracked body.

Since each of the postulated cracks to be analyzed is an axial crack (with respect to the heater sleeve penetration axis), the hoop stresses on the elements representing the crack face are extracted from the stress results and applied in the form of pressure loading.

3.2.3 Calculated and Allowable Stress Intensity Factors

The allowable stress intensity factor was determined for the postulated initial flaw described above. Since the fracture toughness criteria are temperature dependent, evaluations were made for both hot and cold conditions.

The flaw evaluation criteria of Section XI of the ASME Code [5] define the allowable stress intensity factor under normal operating and upset conditions as the material toughness divided by the safety factor of $\sqrt{10}$. Similarly, the safety factor of $\sqrt{2}$ is prescribed for emergency and faulted plant conditions. The pressurizer bottom head is fabricated from low alloy steel SA-533, Grade B, Class 1 material. Therefore, the lower bound fracture toughness curves provided in Appendix A of Section XI can be used to obtain the critical fracture toughness.

The computed maximum stress intensity factor at the overlay-low alloy steel interface under normal/upset conditions was determined, and the transient event during which it occurs was identified, as well as the corresponding temperature. Using that temperature, the critical fracture toughness was calculated and compared to the maximum stress intensity factor. The same procedure was used for the Loss of Secondary Pressure transient, which is the only emergency/faulted condition considered. Table 3-9 shows the maximum stress intensity factors and allowable values for the heater sleeve penetrations.

An ASME Code, Section XI interpretation has been issued regarding the safety factor to be considered at the end of the cooldown transient. If the applied pressure is less than 20% of the Design Pressure (2,500 psia) and the temperature is greater than RT_{NDT} +60°F, then a factor-of-safety of $\sqrt{2}$ may be used instead of $\sqrt{10}$. This results in an allowable stress intensity factor of 47 ksi$\sqrt{in}$ [5] at 70°F at the end of the cooldown transient for an RT_{NDT} of (-)10°F for the Palo Verde low alloy steel base material.

As Table 3-9 shows, all ASME Code allowable stress intensity factor criteria have been satisfied for all loading conditions.

3.3 Elastic-Plastic Fracture Mechanics and Fatigue Crack Growth Evaluations

The controlling loading condition in the foregoing linear elastic fracture mechanics (LEFM) analyses is the Trip at Maximum Pressure Stress event, for which the applied stress intensity factor is 59.2 ksi$\sqrt{in}$ versus an allowable of 63.2 ksi$\sqrt{in}$, as shown in Table 3-9. However, this condition occurs at normal plant operating temperatures, for which the low alloy steel pressurizer base material is on the upper shelf of its Charpy V-notch impact energy curve, and therefore possesses considerable ductility. For low alloy steel components in this temperature regime, elastic-plastic fracture mechanics (EPFM) techniques are more appropriate fracture mechanics technologies than LEFM techniques. The LEFM methodology used above [5] treats all loadings on the vessel equivalently, applying equal safety factors (~3 for normal and upset loads, and ~1.4

for emergency and faulted loads) to both primary stresses, due to internal pressure and mechanical loads, as well as to secondary and peak stresses, such as those caused by differential thermal expansion. These loadings are equivalent in their potential to produce fracture only in the most brittle of materials, such as glass, RPV beltline materials at low temperatures after significant irradiation embrittlement, and thick, ferritic materials at very low temperatures.

Ample precedent exists in the ASME Code, Section XI for the use of EPFM methodologies in materials that exhibit some ductility. Such precedent may be seen in Appendix C for Evaluation of Flaws in Austenitic Piping [5], Appendix H for Evaluation of Flaws in Ferritic Piping [5], and Appendix K for Assessment of Reactor Vessels with Low Upper Shelf Charpy Impact Energy Levels [5]. Appendix H includes a screening criteria to determine into which regime a ferritic piping flaw evaluation falls (LEFM, EPFM or Limit Load), and for problems that fall into the EPFM regime, specifies different safety factors for primary stresses (~3) than for secondary loadings (1). An even more appropriate approach for the pressurizer heater sleeve penetrations is presented in Appendix K [5]. In addition to different safety factors for primary versus secondary loadings, this appendix also provides a procedure for performing flaw instability analysis of reactor vessel materials on the upper shelf, as illustrated schematically in Figure 3-5. The left hand plot in this figure illustrates a typical material J-Resistance (J-R) curve. As loading is applied to the top of a fracture specimen of a ductile material, the J value for that material increases until it exceeds the material fracture toughness, J_{Ic} (similar to K_{Ic} in LEFM evaluations). At this point, if the material is ductile, the crack in the specimen will begin to extend in a slow stable fashion until it reaches the instability point indicated by the upper extent of the J-R curve. For analytical convenience, the material J-R curve may be converted to J versus Tearing Modulus (T), as illustrated in the right hand plot in Figure 3-5. Application of this Tearing Modulus to an engineering component, such as the Palo Verde pressurizer, is then performed by computing J versus T applied for the component, illustrated by the dashed line on the right hand plot. The J-value at which the J-applied line crosses J_{Ic} corresponds to the initiation of slow stable crack propagation. Unstable crack propagation or failure, however, is not predicted until the instability point in the diagram is reached. The difference between $J = J_{Ic}$ versus J at the instability point is a measure of the additional ability to sustain loading afforded by the ductility of the material. In a brittle material, failure occurs at $J = J_{Ic}$ (equivalent to $K = K_{Ic}$ in an LEFM analysis).

In this section, the technical approach and approximate methodology of Appendix K [5] is applied to the Palo Verde pressurizer heater sleeve postulated remnant crack under the Trip at Maximum Pressure Stress event. Safety factors of 3 for primary loads and 1.5 for secondary loads are applied, which are more conservative than those required by Appendices C, H or K. The results indicate considerably more margin to failure, and thus larger allowable crack sizes than the foregoing LEFM analyses.

3.3.1 Material J-Resistance Curve

Appendix K [5] specifies three methods for selection of the material J-integral resistance curve. A J-R curve may be generated by actual testing of the material following accepted test procedures, it may be generated from a J-integral database obtained from the same class of material with the same orientation, or an indirect method of estimating the J-R curve may be used, provided the method is justified for the material. For this analysis, an indirect method is used, based on Charpy V-notch correlations contained in Reference 7.

Figure 3-6, obtained from Reference 7, presents J-T materials curves for irradiated and unirradiated nuclear vessel steels at various upper shelf Charpy V-notch energy levels (in joules). The results show a rough correlation, in that higher J-T curves are generally obtained for higher Charpy V-notch energy levels. An actual correlation curve has been developed (Figure 3-7 and Figure 3-8) between Charpy V-notch energy and the parameters of a J-R curve power law fit of the following form:

$$J = C\,(\Delta a)^{m}$$

In general, a power law fit of this type is only valid for small crack extension (Δa). However, Loss and coworkers [8] have observed good fit for the power law for larger Δa for materials with high upper shelf Charpy energy levels, such as those addressed herein.

Tests of the actual Palo Verde pressurizer base material were conducted in the transverse orientation. These exhibited Charpy V-notch energy levels ranging from a minimum of 98 ft-lbs up to a maximum of 117 ft-lbs at or near the upper shelf temperature (measured at +50°F; the upper shelf temperature is most probably higher than this, and actual upper shelf energies applicable at plant operating temperature are thus expected to be much higher). Thus, the 98 ft-lbs value is used as a conservatively low estimate of the Charpy V-notch upper shelf energy (CVN) level for the Palo Verde pressurizer base material. The CMTR data also provides an average value of the room temperature yield strength of the Palo Verde pressurizer base material of 75.1 ksi, compared to a 50 ksi minimum value from the ASME Code. At 500°F, the yield strength of SA-533, Grade B, Class 1 material is listed at 43.2 ksi in the ASME Code [3]. Therefore, a factored value of 60 ksi is conservatively used in this evaluation.

Based on this CVN of 98 ft-lbs and a flow stress of 80.1 ksi (3.0 Sm), Figure 3-7 and Figure 3-8 are used to determine values of the coefficient "C" and the exponent "m" for the power law J-R curve fit of 5.10 and 0.45, respectively. These have been converted to a J-T diagram, and are illustrated by the "98 ft-lb" J-T curve in Figure 3-9 and Figure 3-10. Additional J-T curves are also presented for an estimated upper shelf Charpy V-notch energy level of 140 ft-lbs [9] and the average CVN upper shelf energy level of 107 ft-lbs for the Palo Verde pressurizer material.

3.3.2 Calculation of Applied J-T

Analyses for J-T applied are performed in accordance with the approximate technique of ASME Code, Section XI, Appendix K. This allows EPFM J-integral estimates to be developed from the foregoing LEFM stress intensity factor calculations. For the Trip at Maximum Pressure Stress event, the resulting stress intensity factors listed in Table 3-9 are:

$$K_{It}\ (\text{Thermal}) = 13.8\ \text{ksi}\sqrt{\text{in}}$$
$$K_{Ip}\ (\text{Pressure}) = 45.4\ \text{ksi}\sqrt{\text{in}}$$
$$K_{Itotal} = 59.2\ \text{ksi}\sqrt{\text{in}}$$

Before proceeding with the EPFM analyses, the screening criteria of Appendix H [5] are applied to demonstrate that the evaluation is in the EPFM regime:

$K_r' = K_{total} / K_{1c} = 59.2/ 200 = 0.296$

$S_r' =$ Peak Stress in Penetration / Flow Stress = 69.7 / 80.1 = 0.87

where the peak stress in the penetration was taken as the maximum stress applied on the crack face.

Thus:

$$SC = K_r' / S_r' = 0.34$$

The Appendix H screening criteria limits are SC ≥ 1.8 for LEFM, 1.8 > SC ≥ 0.2 for EPFM, and SC < 0.2 for Limit Load. Thus, the analysis is clearly in the EPFM regime.

The Appendix K [5] approximate procedure for J-integral involves the calculation of a plastic zone corrected crack size for small scale yielding from elastically calculated K values, in accordance with the following:

$$a_e = a + [1/(6\pi)] [(K_{1p} + K_{1t})/YS]^2$$

The J-integral is then calculated from revised stress intensity factors (K'_{1p} and K'_{1r}) computed at the plastic zone corrected crack size as follows:

$$J = (K'_{1p} + K'_{1r})^2/E'$$

In the above LEFM analyses, stress intensity factors were only calculated for one crack size (0.6"). Therefore, the following approximation was used to determine K's for the plastic zone corrected crack sizes:

$$K' = K\sqrt{(a_e / a)}$$

This approximation, which is based on the assumption that the stress intensity factor (K) is proportional to the square root of the flaw size (a), is conservative since the dominant stresses decrease rather than increase when the crack size becomes larger.

A list of plastic zone size adjusted K' and associated J-applied values, computed in accordance with the above described method, is provided in Table 3-10 and Table 3-11 for the flaw sizes of 0.6" and 1.2", respectively. Results are reported for various combinations of safety factors, as indicated in the first column of the tables, and are plotted as the J-T applied lines in Figure 3-9 and Figure 3-10. Data points are indicated on the J-applied lines with the corresponding values of safety factor (SF) denoted. The instability points in these diagrams correspond to the J-values at which the J-T applied lines intersect the 98 ft-lbs J-T material curves. These occur at 3 in-kips/in^2 for the 0.6" crack size, and at 4 in-kips/in^2 for the 1.2" crack size, which are listed in the last column of Tables 3-10 and 3-11 for comparison with the applied J values.

As discussed above, the appropriate safety factors for normal/upset operating conditions for ductile materials are SF=3 on primary and SF=1.5 on secondary (indicated by the shaded cells in the tables). It is seen that the applied J for both the 0.6" and 1.2" flaw sizes are below the instability limit by a large margin. Therefore, it can be stated that the ASME Code, Section XI allowable flaw size for the Trip at Maximum Pressure Stress event is greater than 1.2".

3.3.3 Fatigue Crack Growth Evaluations

The LEFM methodology of Section XI, Appendix A of the ASME Code [5] was used to perform the fatigue crack growth evaluation.

The fatigue crack growth evaluation used the 40 year number of cycles from Table 3-3. The Loss of Secondary Pressure transient, an emergency/faulted condition transient, was not included in this evaluation. The design transient cycles were assumed to be evenly distributed over the plant lifetime of 40 years. The Cooldown and Reactor Trip transients were each combined with the Heatup transient to form maximum stress intensity factor ranges. Table 3-12 presents the defined cyclic load ranges based on the stress intensity factor values, and corresponding number of cycles for a postulated 60 year life.

To perform the crack growth analysis, the stress intensity factor (K_I) was assumed to be proportional to the square root of the flaw size (a). The K versus "a" distribution was then determined for each transient based on the calculated initial stress intensity factors (K_{Ii}) at the initial flaw size (a_i) using the following equation:

$$K_I = K_{Ii}\sqrt{\frac{a}{a_i}}$$

Table 3-13 presents the K versus "a" distributions for all the transients considered. The initial flaw size, a_i, was taken at the overlay/low alloy steel interface. Using the downhill side of the heater sleeve penetration where the stress intensity factors are the largest, a_i is 0.60 inches.

For the flaw growth through the pressurizer base material, it was assumed that fatigue is the primary propagation mechanism. The ASME Code fatigue crack growth law for carbon and low alloy steels in water environments was used [5]. The crack growth analyses were performed with the **pc-CRACK for Windows** [6] fracture mechanics analysis program.

The fatigue crack growth results are presented in Figure 3-11. The postulated 0.60 inch initial flaw was predicted to grow to a depth of 1.16 inches after 60 years. This end-of-evaluation period flaw is less than the allowable flaw size calculated in Section 3.3.2.

3.4 Corrosion Evaluation of Pressurizer Base Material

The final configuration of the mid-wall repair results in a crevice between the sleeve and the pressurizer base material. This crevice exists for any type of half sleeve repair in the industry (i.e., this condition is not specific to the mid-wall repair). The pressurizer base material consists of SA-533, Grade B, Class 1 low alloy steel, and is therefore subject to corrosion in borated water.

Reference 10, "Low Alloy Steel Component Corrosion Analysis Supporting Small Diameter Alloy 600/690 Nozzle Repair/Replacement Programs", WCAP-15973-P, Rev. 1, has evaluated worst case corrosion conditions and concluded that the minimal amount of corrosion that may occur is well within the acceptable limits identified in Section XI of the ASME Code.

Specifically, WCAP-15973-P, Rev. 1 states that the corrosion rate of the carbon or low alloy steel in the crevice of replaced or repaired nozzles/sleeves that are bounding cases for small diameter Alloy 600 nozzles in Combustion Engineering plants will be approximately 1.53 mils per year (0.00153 inches per year). The bounding case pressurizer heater sleeves have an estimated life of 194 years.

A second evaluation considered the effects of corrosion product buildup in the crevices of bounding case nozzles/sleeves. Corrosion will occupy a greater volume than the material from which they originate. As a result, the crevices will eventually become packed with dense corrosion products that will isolate the steel from the primary water environment. This will cause the corrosion process to be greatly reduced over a period of time. This evaluation estimated that approximately a 0.025 inch increase in hole diameter as a result of corrosion will significantly reduce the corrosion process.

Table 3-1

Load Combinations

Loads	Load Combinations					
	Design	Level A	Level B	Level C	Level D	Test
Pressure (psia)	2500	2550(3)	2550(3)	2250	2250	2250
Temperature (°F)	700	(1)	(1)	(1)	(1)	(2)
Thermal Transients						
Heatup		X	X			
Cooldown		X	X			
Reactor Trip		X	X			

Notes:

1) Varies between 70°F and 653°F.
2) Varies from 120°F to 400°F.
3) Based on the maximum pressure occurring for the Reactor Trip transient.

Table 3-2

Stress Criteria for ASME Code, Class 1 Components

Load Combination	P_m	P_L	$P_L + P_b$	$P_L + P_b + Q$	Notes
Design	1.0 S_m	1.5 S_m	1.5 S_m	-	1
Level A/B	-	-	-	3.0 S_m	1, 2
Level C	Greater of 1.0 S_y or 1.2 S_m	Greater of 1.5 S_y or 1.8 S_m	Greater of 1.5 S_y or 1.8 S_m	-	1, 3
Level D	Greater of 1.0 S_y or 1.2 S_m	Greater of 1.5 S_y or 1.8 S_m	Greater of 1.5 S_y or 1.8 S_m	-	1, 3
Test	0.9 S_y	-	1.35 S_y	-	1, 4

Notes:

1) Alloy 690 material evaluated.
2) The requirements of ASME Code, Section III, Subparagraph NB-3222.4 for peak stresses and cyclic operation must be met.
3) The two service levels were combined in Level C/D, and the allowable of Level C was used.
4) All statically determined membrane stresses resulting from pressure loading were classified as general primary membrane.

Table 3-3

Transients

Event	Cycles[1]
Pressurizer Heatup	500 (750)
Pressurizer Cooldown	500 (750)
Reactor Trip[2]	480 (720)
Plant Leak Test	200 (300)

Notes:
1) Base number is for 40 years of plant operation. Value in parentheses is for 60 years.
2) Includes Loss of Reactor Coolant Flow and Loss of Load.

Table 3-4

Linearized Stress Intensity Results for Controlling Sleeve

Event	Maximum Membrane Stress Intensity (ksi)		Time @ Max Membrane Stress Intensity (sec)		Maximum Mem. + Bending Stress Intensity (ksi)		Time @ Max Mem. + Bending Stress Intensity (sec)	
	Path 1	**Path 2**	**Path 1**	**Path 2**	**Path 1**	**Path 2**	**Path 1**	**Path 2**
Cooldown	13.2	7.9	4408	4408	15.6	9.7	4408	4408
Heatup	6.5	9.2	10494	10494	11.7	11.6	10494	10494
Trip	9.8	5.5	600	600	11.9	7.1	600	600
Pressure[1]	12.4	10.5	N/A	N/A	16.5	12.0	N/A	N/A

Note:
1) Pressure stress intensities as reported are based on a 1,000 psi internal pressure.

Table 3-5

Primary Stress Intensity Evaluation

Load Comb.	Path[1]	Membrane Stress Intensity (ksi)			Membrane + Bending Stress Intensity (ksi)		
		Pressure P_m	Allowable $1.0S_m$[5]	Accept.	Pressure[3] $P_L + P_b$	Allowable $1.5S_m$[5]	Accept.
Design	1	10.5[2]	23.3	Yes	31.1	34.9	Yes
	2	4.0[4]	23.3	Yes	26.3	34.9	Yes
Level C/D	1	10.5[2]	30.6	Yes	31.1	45.9	Yes
	2	4.0[4]	30.6	Yes	26.3	45.9	Yes
Test	1	10.5[2]	29.7	Yes	28.0	44.5	Yes
	2	4.0[4]	29.7	Yes	23.6	44.5	Yes

Notes:
1) Stress paths are shown in Figure 3-3.
2) General primary membrane stress intensity due to pressure was determined by closed form solution. Note that 2,500 psia pressure was conservatively used for Service Level C/D and Test, as well as for Design.
3) Membrane stress intensity from a 1,000 psi unit pressure analysis was scaled to obtain P_L at the Design Pressure of 2,500 psia and Test Pressure of 2,250 psi. $P_b = 0$ for pressure.
4) General primary membrane stress intensity due to pressure was determined via closed form solution for shear in the repair weld along Path 2.
5) Design stress intensity and yield strength for Alloy 690 material per Reference 3 at 700°F.

Table 3-6
Service Level A/B Load Combination
Primary-Plus-Secondary Stress Intensity Evaluation

Path[1]	Membrane + Bending Stress Intensity (ksi)					
	Pressure[2] $P_L + Q$	Cooldown[3] $P_L + Q$	Trip[3] $P_L + Q$	Combined $P_L + Q$	Allowable $3.0S_m$[4]	Accept.
1	42.1	15.6	11.9	69.6	69.9	Yes
2	30.5	9.7	7.1	47.3	69.9	Yes

Notes:
1) Stress paths are shown in Figure 3-3.
2) Membrane-plus-bending stress intensity from a 1,000 psi unit pressure analysis was scaled to obtain $P_L + Q$ at a pressure of 2,550 psia, as this was the maximum pressure experienced under any Service Level A/B load combination (pressure occurs during a Reactor Trip transient).
3) From analysis and post-processing of the Cooldown and Reactor Trip transients. The Heatup stress intensities do not govern and were excluded.
4) Design stress intensity for Alloy 690 material per Reference 3 at 700°F.

Table 3-7

Total Fatigue Usage for Option 1

Path	Location (1)	Region	Fatigue Usage			
			Cooldown+ Trip+ P_{Trip}	Cooldown+ Heatup+ $P_{Operate}$	P_{leak}	Total
1	(I)	Sleeve	0.006	0.000	0.000	0.006
1	(O)	Crevice	0.596	0.023	0.015	0.634
2	(I)	Weld	0.482	0.018	0.022	0.522
2	(O)	Weld	0.262	0.014	0.010	0.286

Note:

1) See Figure 3-3 for illustration of indicated locations.

Table 3-8

Total Fatigue Usage for Option 2

Path	Location (1)	Region	Fatigue Usage			
			Trip+ $P_{Delta\ Trip}$	Cooldown+ Heatup+ $P_{Operate}$	P_{leak}	Total
1	(I)	Sleeve	0.000	0.002	0.000	0.002
1	(O)	Crevice	0.009	0.574	0.015	0.598
2	(I)	Weld	0.005	0.445	0.022	0.472
2	(O)	Weld	0.002	0.347	0.010	0.359

Note:

1) See Figure 3-3 for illustration of indicated locations.

Table 3-9

Stress Intensity Factor Results

Event	Applied Stress Intensity Factor (ksi $\sqrt{in}$)				Allowable Stress Intensity Factor (ksi $\sqrt{in}$)[1]
	Thermal	Internal Pressure	Crack Face Pressure	Total	
Cooldown	25.2	2.9	0.8	28.9	63.2 [3]
End of Cooldown	21.4	1.2	0.3	22.9	47.0 [2]
Trip Max. Thermal Stress	16.5	24.2	7.0	47.7	63.2 [3]
Trip Max. Pressure Stress	13.8	35.2	10.2	59.2	63.2 [3]
Loss of Secondary Pressure	96.9	2.1	0.6	99.6	141.4 [4]

Notes:

1) ASME Code, Section XI acceptance criteria are contained in Paragraph IWB-3612.
2) The allowable stress intensity factor for normal/upset conditions at 70°F is 47.0 $ksi\sqrt{in}$, using a factor-of-safety of $\sqrt{2}$ per the recent ASME Code interpretation with an RT_{NDT} of (-)10°F.
3) The allowable stress intensity factor for normal/upset "hot" conditions is 63.2 $ksi\sqrt{in}$.
4) The allowable stress intensity factor for emergency/faulted "hot" conditions is 141.4 $ksi\sqrt{in}$.

Table 3-10

J-T Instability Computations for Palo Verde Pressurizer Remnant Crack using ASME Code, Section XI, Appendix K Approximate Method, Initial Flaw Size of 0.6"

Safety Factors	K_{total}	K'_{total}	J'_{total}	T'	J @ Instability
	ksi$\sqrt{in}$		in-kips/in^2		in-kips/in^2
SF=1	59.2	61.7	0.119	0.900	3.00
SF=3, 1.5	156.9	198.8	1.231	9.338	3.00
SF=$\sqrt{10}$	187.2	255.4	2.032	15.416	3.00
SF=4	236.8	365.1	4.154	31.511	3.00
SF=5	296.0	525.5	8.606	65.281	3.00

Table 3-11

J-T Instability Computations for Palo Verde Pressurizer Remnant Crack using ASME Code, Section XI, Appendix K Approximate Method, Extended Flaw Size of 1.2"

Safety Factors	K_{total}	K'_{total}	J'_{total}	**T'**	**J @ Instability**
	ksi$\sqrt{in}$		**in-kips/in^2**		**in-kips/in^2**
SF=1	83.7	87.3	0.237	0.900	4.0
SF=3, 1.5	221.9	281.1	2.462	9.338	4.0
SF=$\sqrt{10}$	264.8	361.1	4.065	15.416	4.0
SF=4	334.9	516.3	8.309	31.511	4.0
SF=5	418.6	743.2	17.213	65.281	4.0

Table 3-12

Crack Growth Evaluation Cyclic Loads

Load Range	**Cycles**
Reactor Trip – Heatup	720
Cooldown – Heatup	30
Leak Test	300

Table 3-13

Stress Intensity Factor vs. Crack Size

a, in.	K (ksi-in$^{1/2}$)			
	Heatup	Cooldown	Trip	Leak Test
0.600	-18.8	28.9	59.2	40.1
0.615	-19.0	29.2	59.9	40.5
0.630	-19.3	29.6	60.7	41.0
0.645	-19.5	29.9	61.4	41.5
0.660	-19.7	30.3	62.1	42.0
0.675	-19.9	30.6	62.8	42.5
0.690	-20.2	31.0	63.5	42.9
0.705	-20.4	31.3	64.2	43.4
0.720	-20.6	31.6	64.8	43.9
0.735	-20.8	32.0	65.5	44.3
0.750	-21.0	32.3	66.2	44.8
0.765	-21.2	32.6	66.8	45.2
0.780	-21.4	32.9	67.5	45.7
0.795	-21.6	33.2	68.1	46.1
0.810	-21.8	33.6	68.8	46.5
0.825	-22.0	33.9	69.4	47.0
0.840	-22.2	34.2	70.0	47.4
0.855	-22.4	34.5	70.7	47.8
0.870	-22.6	34.8	71.3	48.2
0.885	-22.8	35.1	71.9	48.6
0.900	-23.0	35.4	72.5	49.1
0.915	-23.2	35.7	73.1	49.5
0.930	-23.4	36.0	73.7	49.9
0.945	-23.6	36.2	74.3	50.3
0.960	-23.8	36.5	74.9	50.7
0.975	-24.0	36.8	75.5	51.1
0.990	-24.1	37.1	76.0	51.4
1.005	-24.3	37.4	76.6	51.8
1.020	-24.5	37.7	77.2	52.2
1.035	-24.7	37.9	77.7	52.6
1.050	-24.9	38.2	78.3	53.0
1.065	-25.0	38.5	78.9	53.4
1.080	-25.2	38.7	79.4	53.7
1.095	-25.4	39.0	80.0	54.1
1.110	-25.6	39.3	80.5	54.5
1.125	-25.7	39.5	81.0	54.8
1.140	-25.9	39.8	81.6	55.2
1.155	-26.1	40.1	82.1	55.6
1.170	-26.3	40.3	82.7	55.9
1.185	-26.4	40.6	83.2	56.3
1.200	-26.6	40.8	83.7	56.6

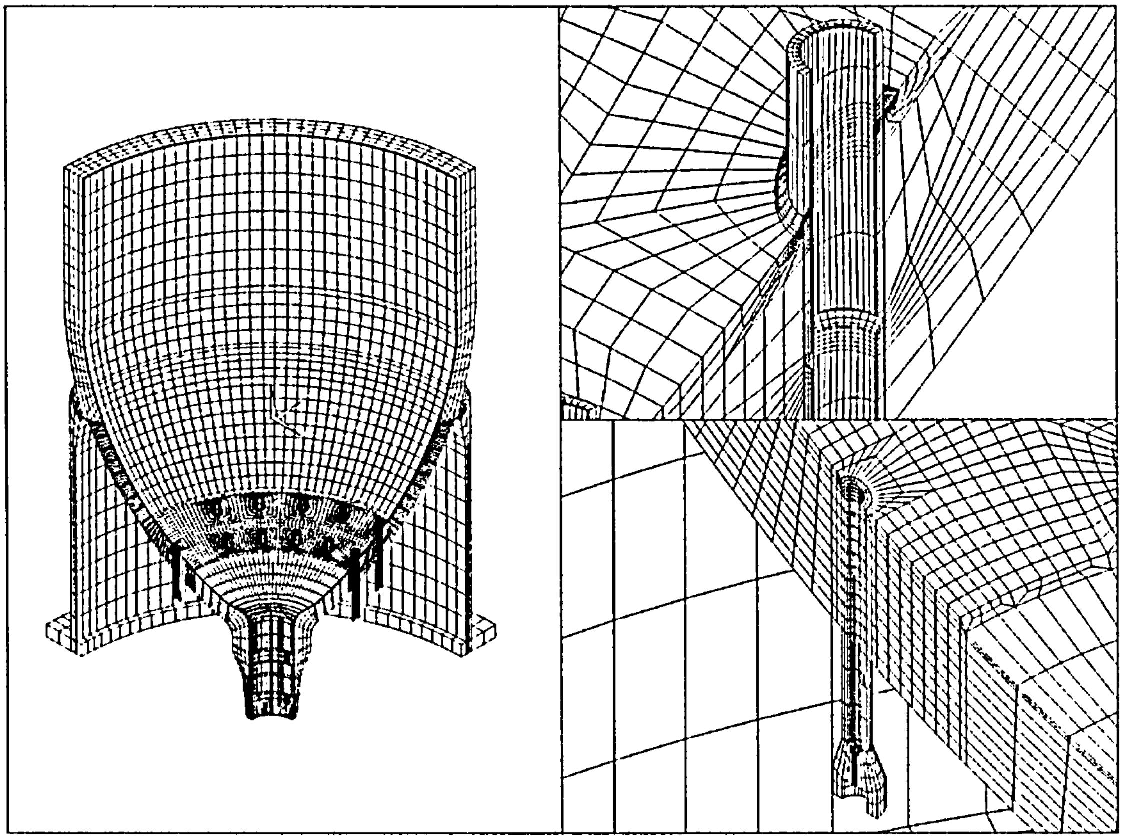

Figure 3-1. Finite Element Model

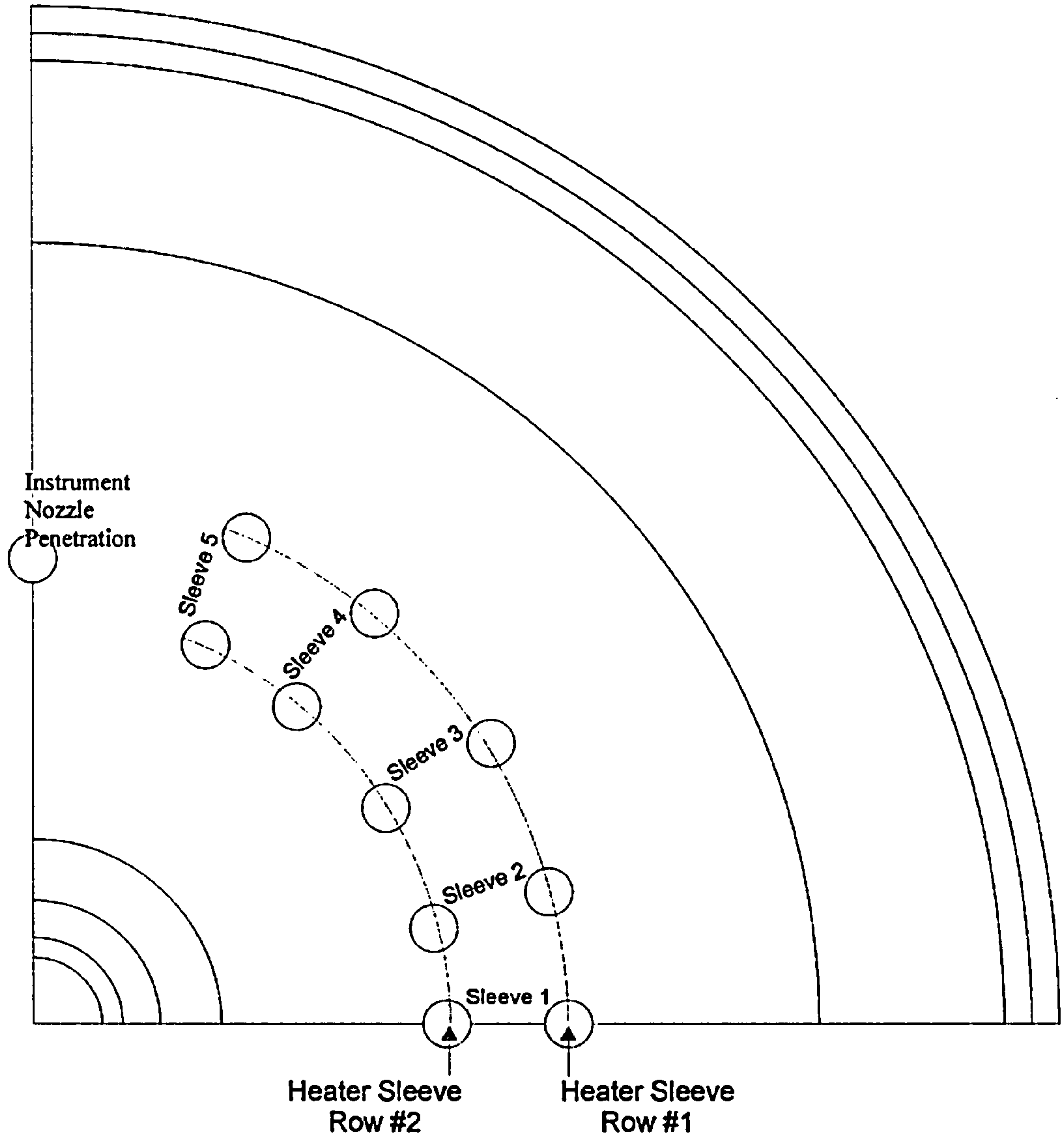

Figure 3-2. Row and Sleeve Numbering

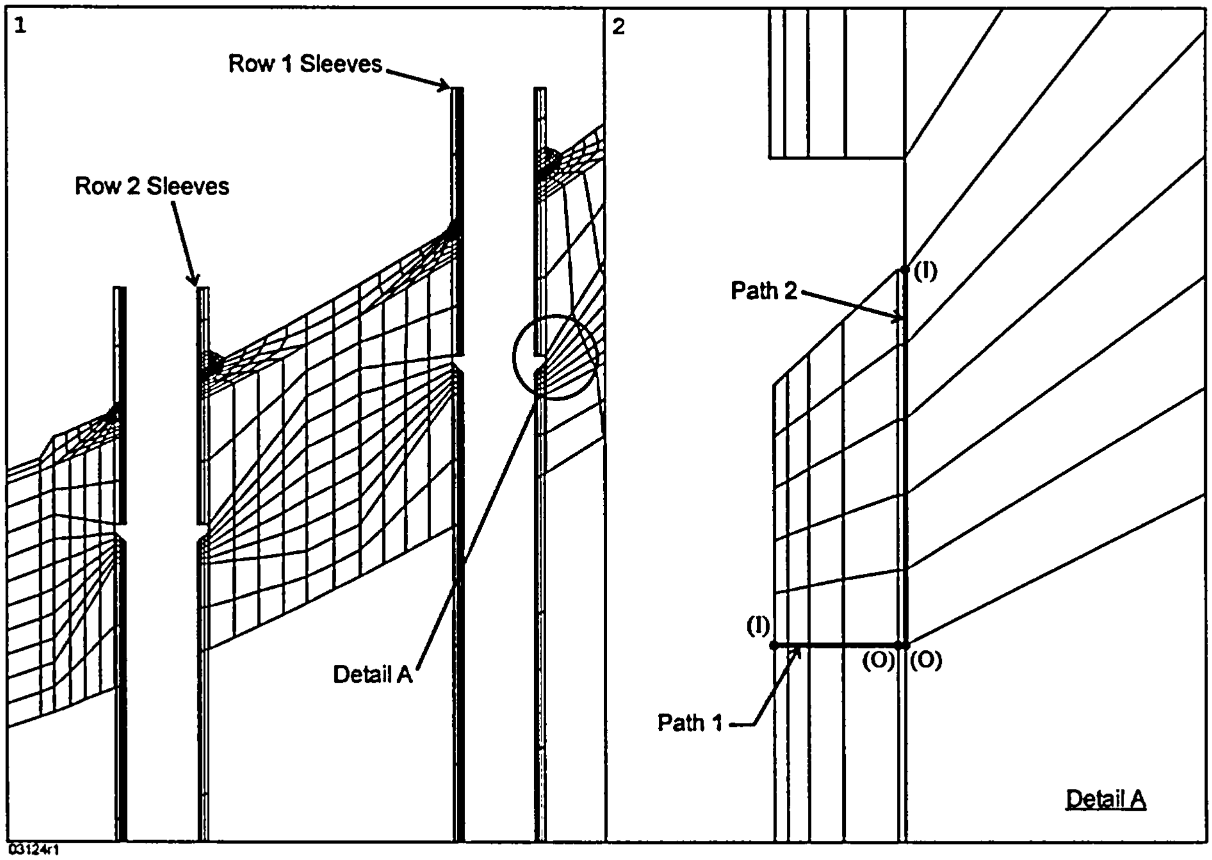

Figure 3-3. Linearized Stress Paths for Sleeve Repairs

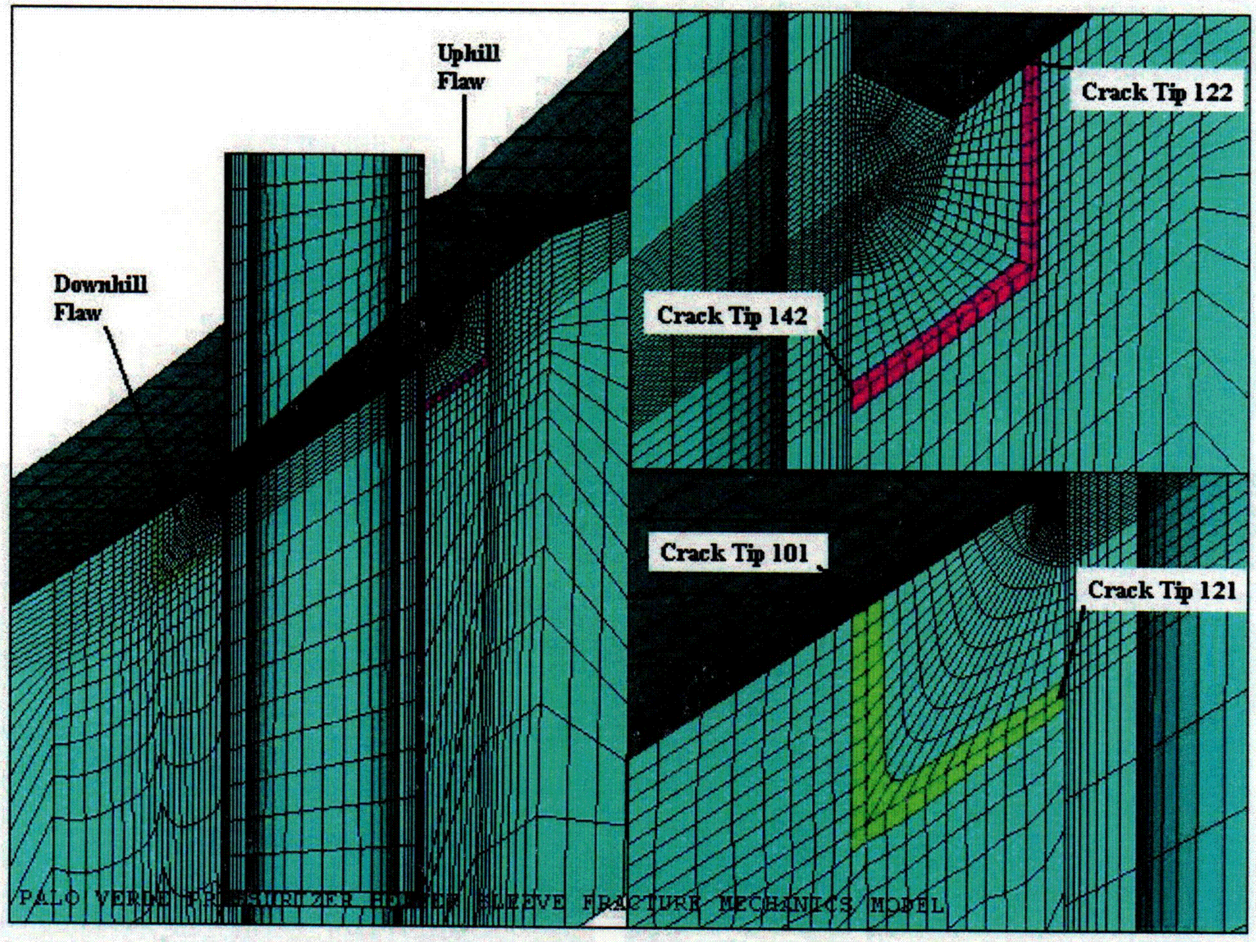

Figure 3-4. Crack Tip Element Location Definition

C01

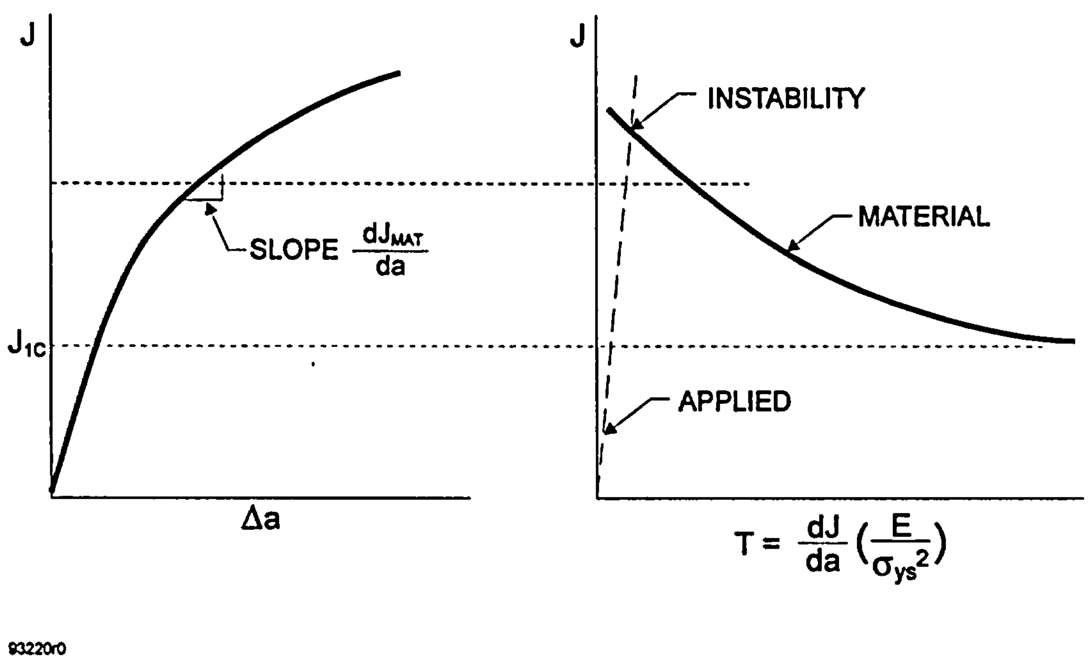

Figure 3-5. Schematic of EPFM Stability Analysis from ASME Code, Section XI, Appendix K [5]

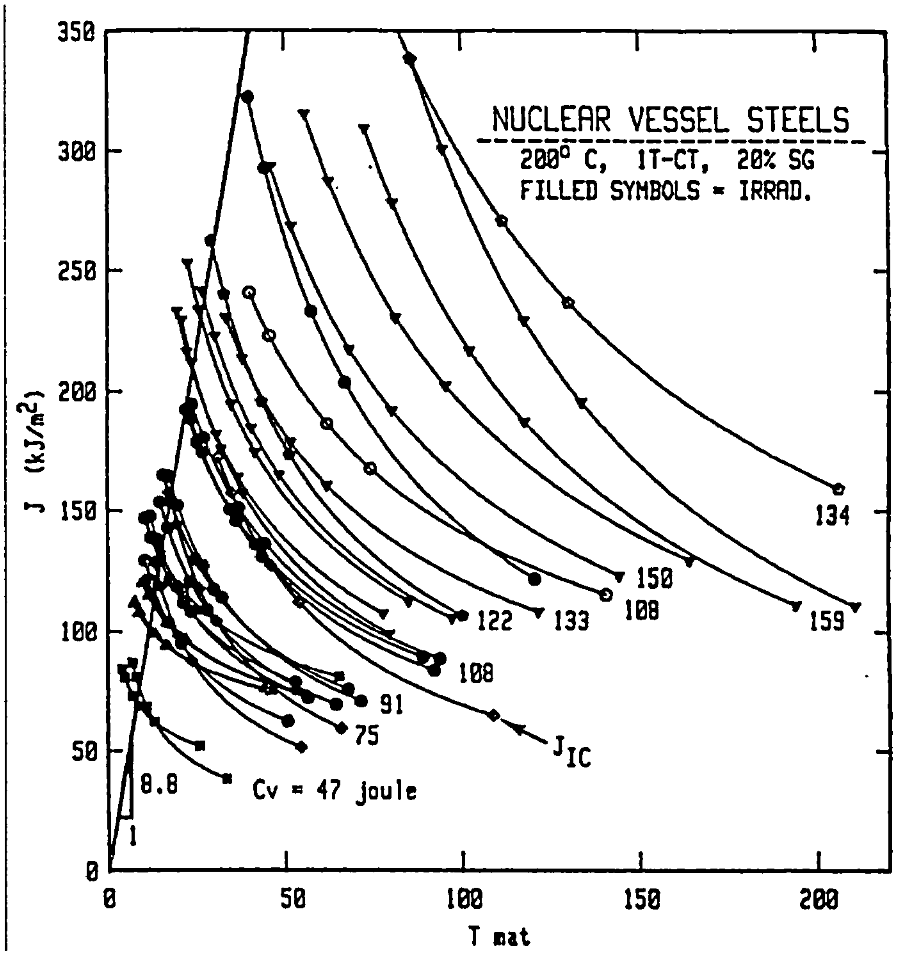

Figure 3-6. J-T Diagram for Several Reactor Vessel Steels and Welds Showing Rough Correlation with Charpy V-notch Upper Shelf Energy [7]

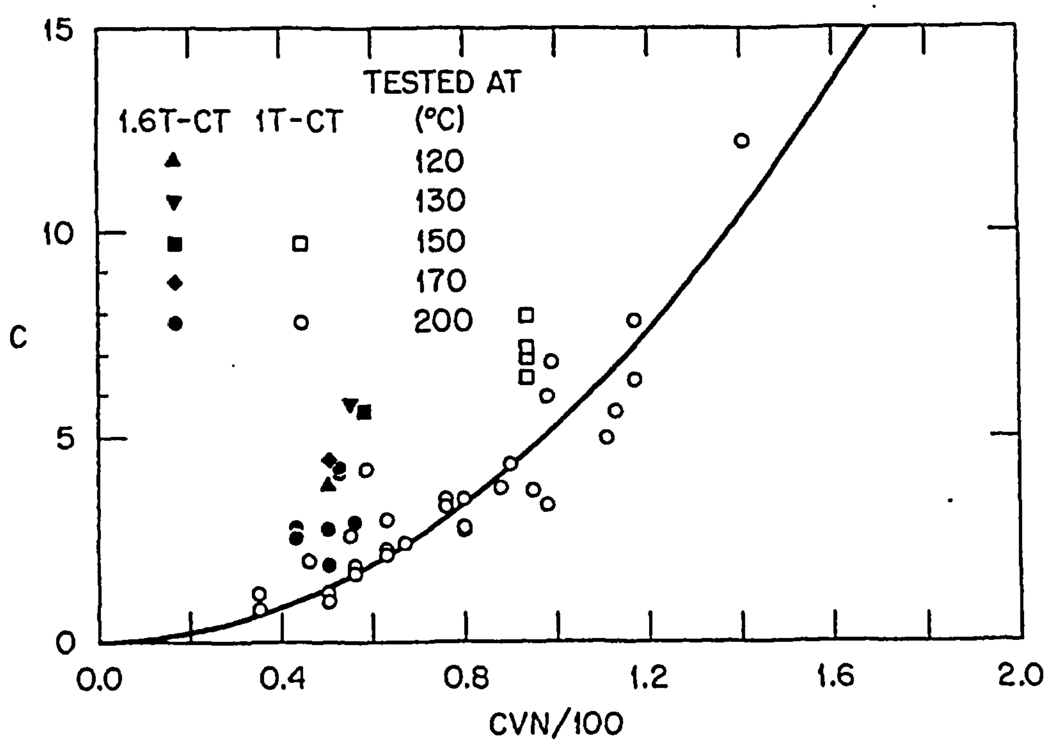

Figure 3-7. Correlation of Coefficient C of Power Law J-R Curve Representation with Charpy V-notch Upper Shelf Energy [7]

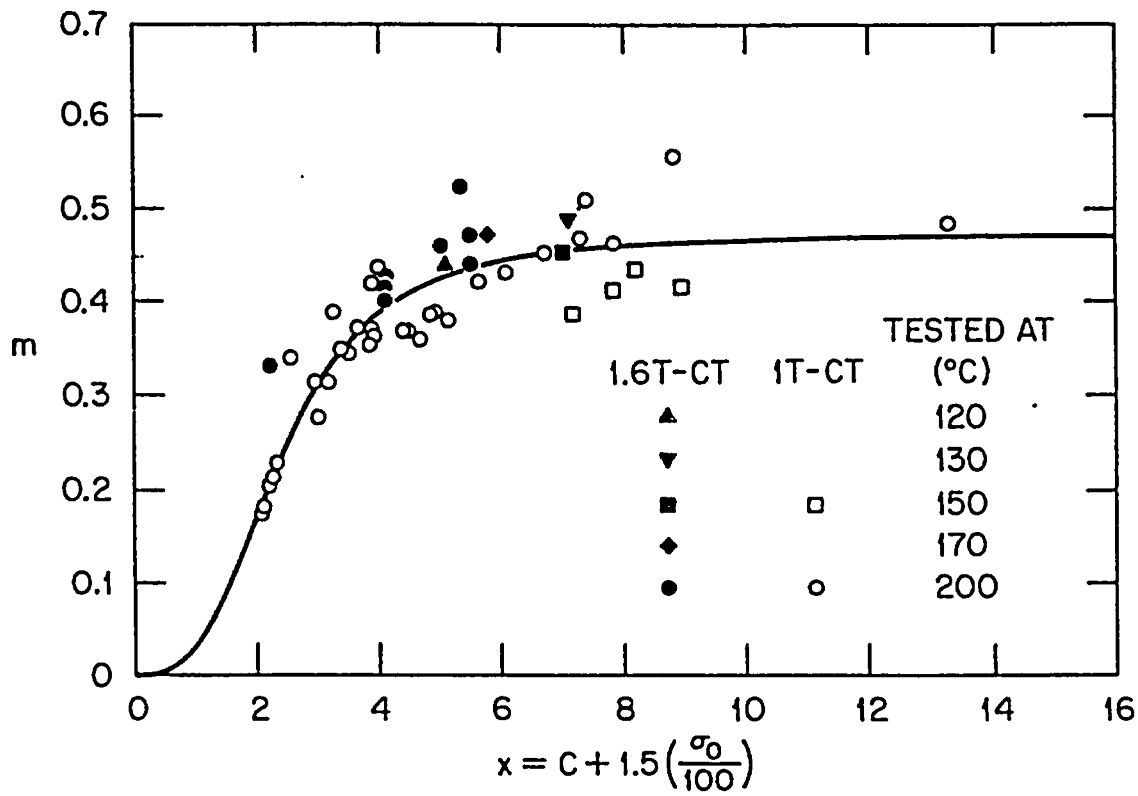

Figure 3-8. Correlation of Exponent m of Power Law J-R Curve Representation with Coefficient C and Flow Stress σ_o [7]

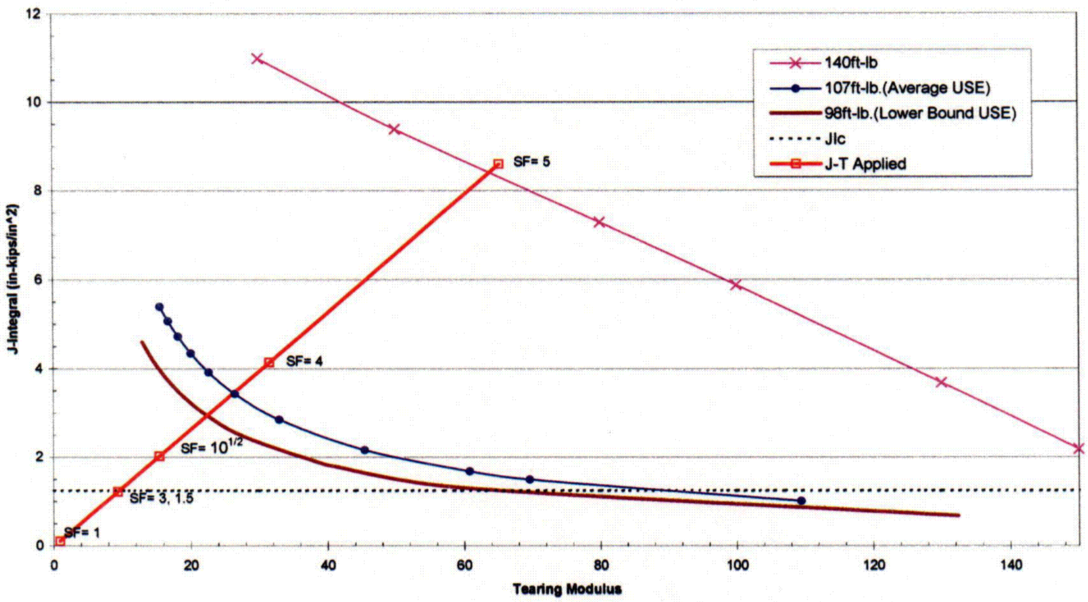

Figure 3-9. J-T Diagram for EPFM Stability Analysis for Palo Verde Pressurizer Remnant Cracking Concern at a Flaw Size of 0.6"

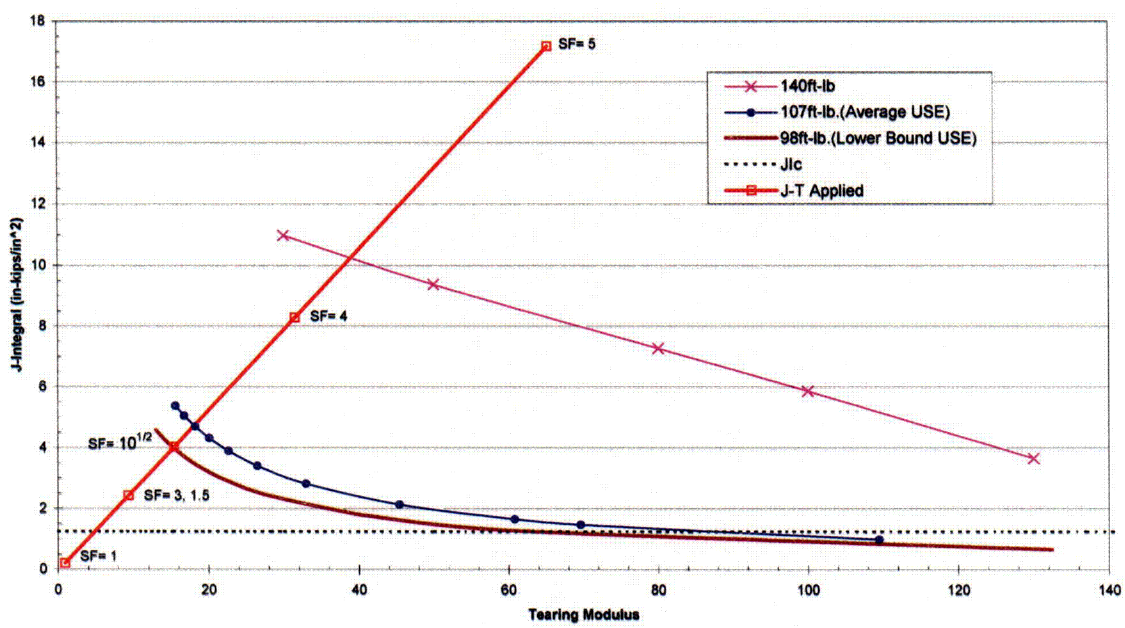

Figure 3-10. J-T Diagram for EPFM Stability Analysis for Palo Verde Pressurizer Remnant Cracking Concern at a Flaw Size of 1.2"

C02

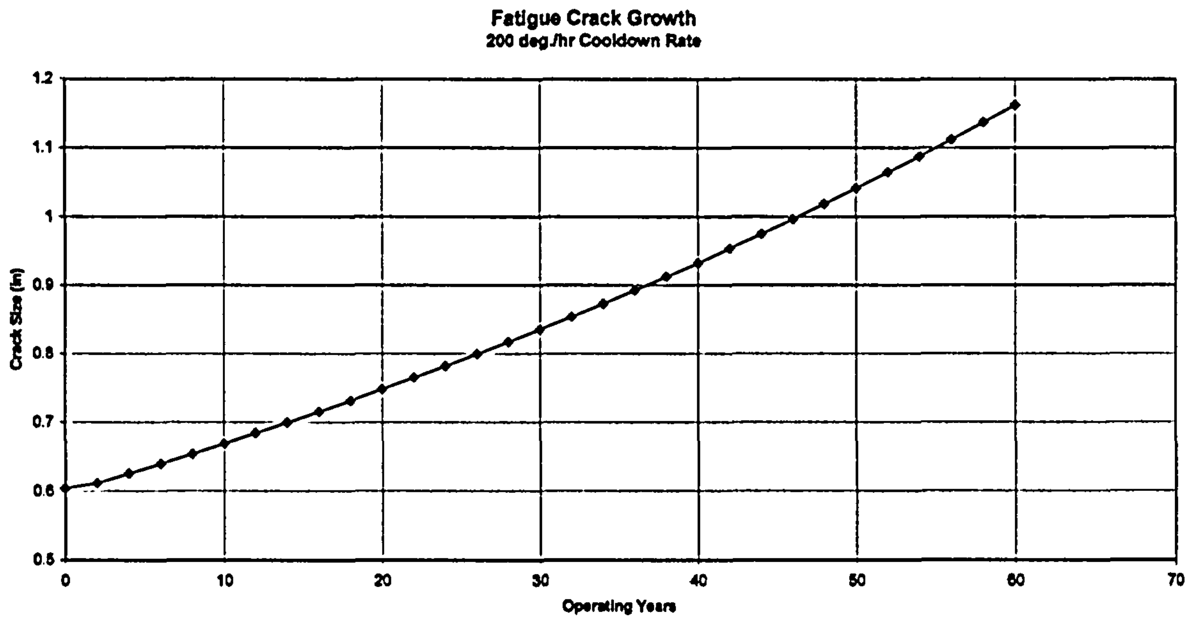

Figure 3-11. Fatigue Crack Growth Results

4.0 CONCLUSIONS

The proposed pressurizer heater sleeve mid-wall repair concept is acceptable because:

- The design of the heater sleeve repair meets the requirements of ASME Code, Section III.
- The remaining postulated defect in the Alloy 600 material has been evaluated and found acceptable for the life of the plant plus life extension.
- Postulated wall loss due to corrosion of base material is minimal.

5.0 REFERENCES

1. ANSYS Mechanical, Revision 5.7, ANSYS Inc., December 2000.

2. ASME Boiler and Pressure Vessel Code, 1971 Edition through Winter 1973 Addenda.

3. ASME Boiler and Pressure Vessel Code, Section III, Appendices, 1989 Edition.

4. T. L. Anderson, "Fracture Mechanics Fundamentals and Applications", Second Edition, CRC Press, 1995.

5. ASME Boiler and Pressure Vessel Code, Section XI, 1992 Edition, including the 1992 Addenda. For references to Appendix K, see the 1993 Addenda.

6. pc-CRACK for Windows, Version 3.1-98348, Structural Integrity Associates, 1998.

7. NUREG-0744, Vol. 2, Rev. 1, "Resolution of the Task A-11 Reactor Vessel Materials Toughness Safety Issue," Appendices C-K, Division of Safety Technology, Office of Nuclear Reactor Regulation, U.S. Nuclear Regulatory Commission, Washington, D.C. 20555, October 1982.

8. F. Loss, ed., "Structural Integrity of Water Reactor Pressure Boundary Components," USNRC Report NUREG/CR-1128, 1979.

9. S.S. Tang, P.C. Riccardella, and R. Huet, "Verification of Tearing Modulus Methodology for Application of Pressure Vessels with Low Upper Shelf Fracture Toughness," presented at ASTM 2nd International Symposium on Elastic-Plastic Fracture Mechanics, October 6-9, 1981, Philadelphia, PA.

10. WCAP-15973-P, Rev. 1, "Low Alloy Steel Component Corrosion Analysis Supporting Small Diameter Alloy 600/690 Nozzle Repair/Replacement Programs."

Attachment 2

ASME Technical Interpretation IN 03-013

Codes and Standards

ASME International

Three Park Avenue
New York, NY 10016-5990
U.S.A.

September 8, 2003

Joseph G. Weicks
JWEICKS@entergy.com

Subject: Technical Interpretation

File #: IN 03-013

Applicability: 1989 Edition through the 2001 Edition with the 2003 Addenda

Dear Mr. Weicks:

Our understanding of the question in your letter and our reply is as follows:

Question: Does Section XI permit the application of the criteria of IWB-3613(a) to structural discontinuities at the intersections of nozzles and pressure vessel shells during conditions where pressurization does not exceed 20 percent of the Design Pressure?

Reply: Yes.

Sincerely,

Oliver Martinez

Oliver Martinez, Secretary
SC XI Interpretation Committee
212-591-7005
212-591-8502 fax
Martinezo@asme.org

CC: Joel Feldstein
Richard Gimple
William Holston
Guido Karcher